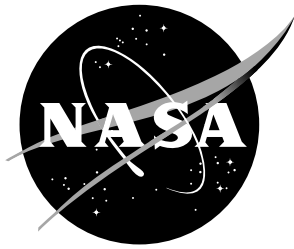


NASA/TM-2016-219278



Initial Report on International Space Station Radiation Environment Monitor Performance

Nicholas Stoffle, Ph.D.
Leidos - Houston, Texas, USA

John Keller
KBRwyle - Houston, Texas, USA

Edward Semones
NASA Johnson Space Center - Houston, Texas, USA

September 2016

NASA STI Program... in Profile

Since its founding, NASA has been dedicated to the advancement of aeronautics and space science. The NASA scientific and technical information (STI) program plays a key part in helping NASA maintain this important role.

The NASA STI Program operates under the auspices of the Agency Chief Information Officer. It collects, organizes, provides for archiving, and disseminates NASA's STI. The NASA STI Program provides access to the NASA Aeronautics and Space Database and its public interface, the NASA Technical Report Server, thus providing one of the largest collections of aeronautical and space science STI in the world. Results are published in both non-NASA channels and by NASA in the NASA STI Report Series, which includes the following report types:

- **TECHNICAL PUBLICATION.** Reports of completed research or a major significant phase of research that present the results of NASA programs and include extensive data or theoretical analysis. Includes compilations of significant scientific and technical data and information deemed to be of continuing reference value. NASA counterpart of peer-reviewed formal professional papers, but having less stringent limitations on manuscript length and extent of graphic presentations.
- **TECHNICAL MEMORANDUM.** Scientific and technical findings that are preliminary or of specialized interest, e.g., quick release reports, working papers, and bibliographies that contain minimal annotation. Does not contain extensive analysis.
- **CONTRACTOR REPORT.** Scientific and technical findings by NASA-sponsored contractors and grantees.

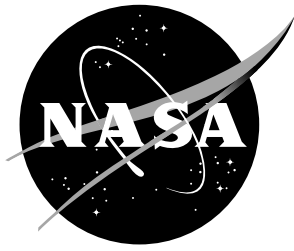
- **CONFERENCE PUBLICATION.** Collected papers from scientific and technical conferences, symposia, seminars, or other meetings sponsored or co-sponsored by NASA.
- **SPECIAL PUBLICATION.** Scientific, technical, or historical information from NASA programs, projects, and missions, often concerned with subjects having substantial public interest.
- **TECHNICAL TRANSLATION.** English-language translations of foreign scientific and technical material pertinent to NASA's mission.

Specialized services also include organizing and publishing research results, distributing specialized research announcements and feeds, providing information desk and personal search support, and enabling data exchange services.

For more information about the NASA STI Program, see the following:

- Access the NASA STI program home page at <http://www.sti.nasa.gov>
- E-mail your question to help@sti.nasa.gov
- Phone the NASA STI Information Desk at 757-864-9658
- Write to:
NASA STI Information Desk
Mail Stop 148
NASA Langley Research Center
Hampton, VA 23681-2199

NASA/TM-2016-219278



Initial Report on International Space Station Radiation Environment Monitor Performance

Nicholas Stoffle, Ph.D.
Leidos - Houston, Texas, USA

John Keller
KBRwyle - Houston, Texas, USA

Edward Semones
NASA Johnson Space Center - Houston, Texas, USA

National Aeronautics and
Space Administration
Johnson Space Center

September 2016

Acknowledgments

The authors would like to acknowledge the REM Science Team at NASA JSC and at the University of Houston for contributing to the success of the REM deployment and operation, as well as the JSC Flight Control Team (PLUTO, OCA, Ops Plan) and Payload Team (JSC-PIM, MSFC-POD, OC, Ops Team) for their help in hardware readiness, deployment, and operations.

This work was supported by the NASA Advanced Exploration Systems Program and NASA Bioastronautics Contract NAS9-02078. Contributions were also made by the University of Houston through Wyle Science Technology and Engineering Group contract number T72203.

<p>The use of trademarks or names of manufacturers in this report is for accurate reporting and does not constitute an official endorsement, either expressed or implied, of such products or manufacturers by the National Aeronautics and Space Administration.</p>

Available from:

NASA Center for AeroSpace Information
7115 Standard Drive
Hanover, MD 21076-1320

National Technical Information Service
5301 Shawnee Road
Alexandria, VA 22312

Available in electronic form at <http://ston.jsc.nasa.gov/collections/TRS>

Abstract

The International Space Station Radiation Environment Monitor (ISS REM) is a small, low-power, hybrid-pixel radiation detector based on the CERN Timepix technology. Five detectors were flown aboard ISS beginning in late 2012. This document contains the initial results from the first year of operation as reviewed in late 2013, including hardware issues, detector performance, and development efforts.

1 Introduction

The ISS Radiation Environment Monitor (ISS REM) project, launched aboard 48P on August 01, 2012, consists of a set of 5 solid-state pixel-based radiation detection devices coupled with flight software operating on Station Support Computers (SSCs). ISS REM hardware units were deployed on October 16, 2012 (GMT 2012/290). The REM hardware is based on the Medipix2 technology developed at CERN and adapted for Space Radiation monitoring use employing the Timepix version of the Medipix2 Technology¹.

Each of the REM units consist of a Timepix read-out chip bonded to a 300 μm thick, 2 cm^2 silicon sensor layer. The Timepix provides on-chip data collection and signal digitization within the footprint of each of the individual pixels in the 256 by 256 pixel matrix. The Timepix detectors provide energy deposition and related position information, allowing direction information to be derived for particle tracks traversing the silicon sensor layer.

The ISS REM flight software is based on the Pixelman software², and was developed in collaboration with the University of Houston Physics Department and the Institute for Experimental and Applied Physics at the Czech Technical University in Prague. The software provides acquisition and readout control of the Timepix chip, and includes algorithms to automatically adjust data acquisition parameters, perform file transfer to and from ISS file servers, and initiate acquisition software restarts without crew interaction. The adjustment of acquisition parameters for the ISS REM units allows efficient use of available file space while ensuring adequate separation of particle track data during transits through high particle flux regions of the orbit such as the South Atlantic Anomaly (SAA).

The two images in figure 1 are examples of ISS REM data frames for passes through the SAA and through high latitude regions. Note that the data acquisition times for the frames are very different, and the acquisition time adjustment is required due to variations in particle flux encountered within the ISS orbit.

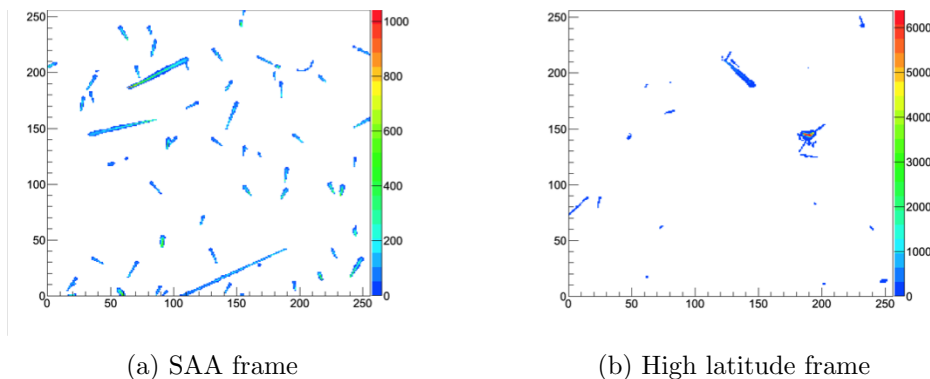


Figure 1: Example data frames for SAA and High Latitude regions of the ISS orbit.

¹See <http://medipix.web.cern.ch> for details on the CERN Medipix and Timepix technology

²The Pixelman software suite was developed and is maintained by the Institute for Experimental and Applied Physics at the Czech Technical University in Prague (IEAP). See <http://aladdin.utef.cvut.cz/ofat/others/Pixelman/> for details on the Pixelman software.

2 Operation Status

2.1 Status as of September 24, 2013

The ISS Radiation Environment Monitor flight software is designed to accommodate both instrument upsets resulting in communication interruption between the USB hardware and the flight software, as well as nominal SSC reboots which are scheduled weekly. Upon crew login to the SSC workstation, the ISS REM software reinitializes communication with the ISS REM hardware and resumes data acquisition without crew interaction.

REM S/N	REM CHIP-ID	SSC	ISS Module	CURRENT STATUS	SSC Status
1003	I04-W0094	SSC 4	Node 1	Data received up to Sept 24/1646 GMT	
1004	E06-W0087	SSC 17	Cupola	Data last received Feb 28/1426 GMT	REM unit remains unresponsive. 35S Return on Nov 11 (In-Work)
1005	I03-W0094	SSC 16	US Lab	Data received up to Sept 22/0725 GMT	SSC restart expected to reinitialize device
1007	D03-W0094	SSC 7	Node 2	Data received up to Sept 24/1648 GMT	
1009	G03-W0094	SSC 15	JPM	Data received up to Sept 24/1647 GMT	

Figure 2: ISS REM status as of September 24, 2013.

2.2 Operational History

On GMT 2012/290, the ISS REM hardware was deployed to selected SSCs. All five ISS REM units were deployed; however, during deploy of the 5th unit (SN 1009) on SSC15, the software's Graphical User Interface failed to display dose information. The ISS REM flight software indicated the hardware for SN 1009 was operating nominally, and ISS REM deploy activities were completed despite the lack of dose display. Further investigation revealed missing configuration files for ISS REM unit SN 1009 in the on-orbit software load, and plans were put in work to uplink the required files. On GMT 2012/291, the crew observed a full hard drive on SSC15 along with error messages relating to the ISS REM software. The crew attempted to restart the software but error messages persisted, and the crew subsequently shut down the ISS REM software. The ISS REM configuration files were cleared by ground teams, and configuration files for ISS REM SN 1009 were uplinked to the SSCs on GMT 2012/291.

Due to the missing calibration files, the ISS REM flight software wrote uncalibrated data to the hard drive on SSC15 at the maximum defined acquisition rate. In addition, without the proper configuration information, the nominal transfer and subsequent delete operations carried out when the flight software moves files to the downlink folder on the server were not performed for ISS REM SN 1009. The uplink of configuration files on GMT 2012/291 and deletion of uncalibrated ISS REM data on SSC15 resolved the issues related ISS REM SN 1009 and the subsequent "disk full" errors on SSC15.

Modified configuration files were uplinked on GMT 2012/297 to reduce the pixel occupancy parameters on all units. This modification increased track separation during SAA passes, and provided for higher quality data for use in dose analysis.

Modifications to configuration files were made for all units and uplinked on GMT 2012/299 to limit the amount of data written to a single log file and to modify REM acquisition parameters to allow for better adjustment of data acquisition rates during transits through the SAA.

Configuration file updates were uplinked on GMT 2012/307 and GMT 2012/318 to further refine the ISS REM acquisition parameters. A small number of temporally separated, high pixel occupancy frames were noted during SAA passes. The level of pixel occupancy in such frames resulted in a high degree of particle track overlap. The software parameters causing the unwanted variation in acquisition time were identified and updated to allow for a smoother transition in acquisition parameters during SAA passes.

Configuration files uplinked on GMT 2013/194 increased the bias voltage on all deployed units from 14.5 volts to 35 volts. This was done to ensure the full 300 μm width of the silicon sensor layer was in a charge depleted state and was expected to provide for more efficient charge collection within the ISS REM sensor layer.

The ISS REM Uplink Log in Appendix A provides detailed information on configuration changes. Appendix B contains information on SSC configuration and ISS REM data flow.

ISS REM SN 1004 stopped recording data on GMT 2013/059. Troubleshooting included verification that the Flight Software was operational, verification that the proper configuration files were present, verification that the device was seated securely in the USB port, and verification that the driver software on the SSC was deployed. The hardware experienced several nominal SSC reboots, and the SSC restarts did not successfully reinitialized the device. An operational change request (OCR) was approved through Payloads to move ISS REM SN 1004 to SSC17 in the Cupola in order to verify that the issue was not related to SSC13 hardware, with verified configuration files uplinked for ISS REM SN 1004 on GMT 2013/101 to ensure the fault was not related to corrupted configuration files. The ISS REM flight software on SSC17 did not recognize ISS REM SN 1004, and the unit was declared unresponsive and was scheduled for return on 35S for further investigation into the cause of the hardware failure.

3 Analysis Summary

REM Summary Information - GMT 2012/320 to GMT 2013/045 (Nov 15, 2012 to Feb 14, 2013 or ~90days)							
S/N	Chip-ID	Live Time [d:h:m:s]	Avg Dose Rate (uGy/day)	Avg Dose Equiv Rate (uSv/day)	Total Dose [uGy]	Total Dose Equiv [uSv]	Q_{eff}
1003	I04-W0094	78:19:57:27.35	298.16	655.79	23504.81	51696.58	2.20
1004	E06-W0087	49:07:46:37.26	273.99	679.38	13514.08	33509.93	2.48
1005	I03-W0094	75:20:57:16.62	221.34	510.22	16794.11	38711.69	2.31
1007	D03-W0094	61:00:30:59.33	253.45	639.56	15465.94	39027.00	2.52
1009	G03-W0094	47:18:46:18.52	382.84	864.22	18292.92	41294.10	2.26

Figure 3: Analysis summary of ISS REM data for approximately 90 days of operation

The ISS REM data analysis summary covers a period of approximately 90 days, beginning on November 15, 2012. ISS REM data is consistent with data taken by other instruments in the Low Earth Orbit (LEO) radiation environment. Differentiation of trapped radiation from Galactic Cosmic Ray (GCR) and other components of the radiation field is also possible based on ISS REM data.

The REM Summary Information table in figure 3 displays the differences in the average dose rate and average dose equivalent rates between the individual ISS REM units. These differences are also present in the plots that follow, and the differences of values within in the summary table are consistent with the ensuing data analysis and discussion. Investigation is in progress to evaluate the root cause of these differences, be it shielding, directionality of the trapped radiation relative to the detectors, or other characteristics of the radiation field or detectors.

4 Plots and Discussion

4.1 Detector Live Time, Operation, and Measured Dose Rate

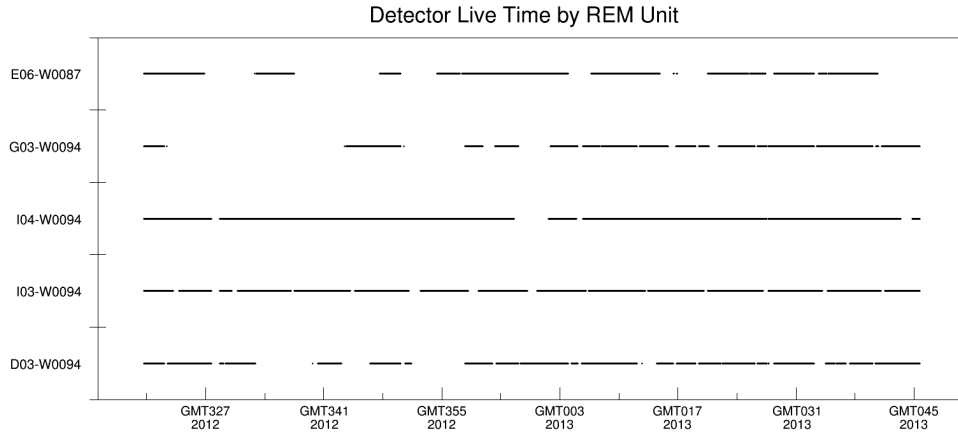


Figure 4: Unit live time for the 90-day analysis period. Missing data is primarily the result of SSC downtime.

Overall, the ISS REM units have performed at or beyond expectations. Aside from the loss of data described in the Operational History section for ISS REM SN1004 (Chip-ID E06-W0087), the hardware has functioned without significant problems since initial deployment, and only minor issues have been encountered in that time. These issues have been related either to configuration settings or to SSC issues independent of the ISS REM flight software or hardware. Acquisition time adjustment algorithms have been operating very well with a minimal number of parameter changes necessary to provide good track separation during SAA transits.

The ISS REM hardware has a very large dynamic range and can acquire individual data frames with durations on the order of microseconds through minutes or longer; however, the device is limited to a maximum readout cadence of 5 frames per second due to the USB interface employed by the hardware. The time required for the software to interact with the hardware is determined by the USB interface speed and is not included in live time calculations. This detector dead time is on the order of a few tenths of a second per data frame, and as a result, even a perfectly operating detector will not have a live time exactly equal to the analysis period length.

The plots of per-data-frame dose rates and dose equivalent rates as a function of time in figures 5 through 9 show the live time of the respective detectors in addition to the dose rates seen in each data frame during operation throughout the analysis period. Data gaps are visible where ISS REM flight software was not collecting data. In the event that an SSC loses connection, data is stored locally on the SSC until network connection is reestablished, and acquired data can then be transferred to the file server, so any data loss shown is related to time periods when the ISS REM flight software was not running on the associated SSC.

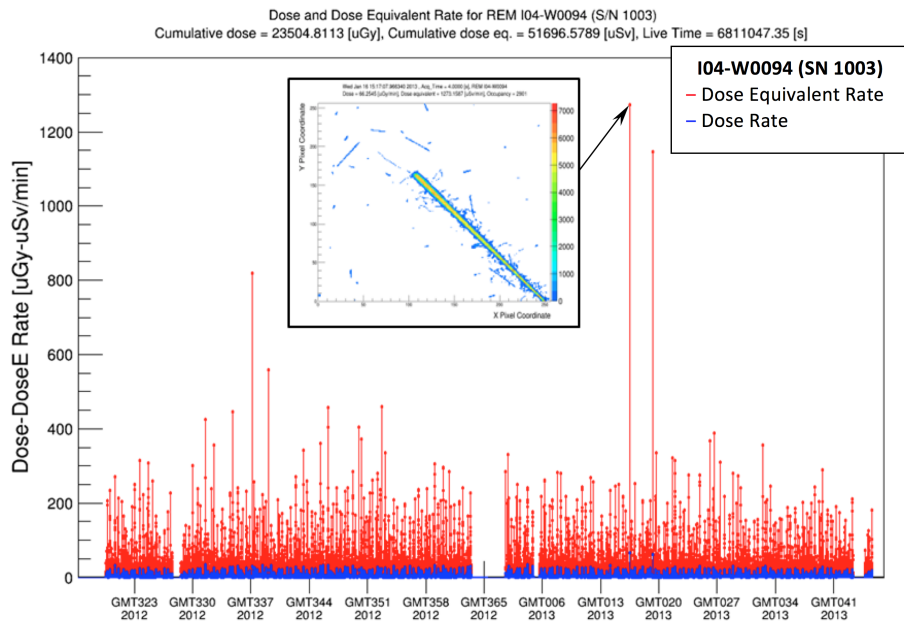


Figure 5: SN 1003 dose rate and dose equivalent rate as a function of time. The inset shows a frame corresponding to the indicated high dose equivalent rate data point.

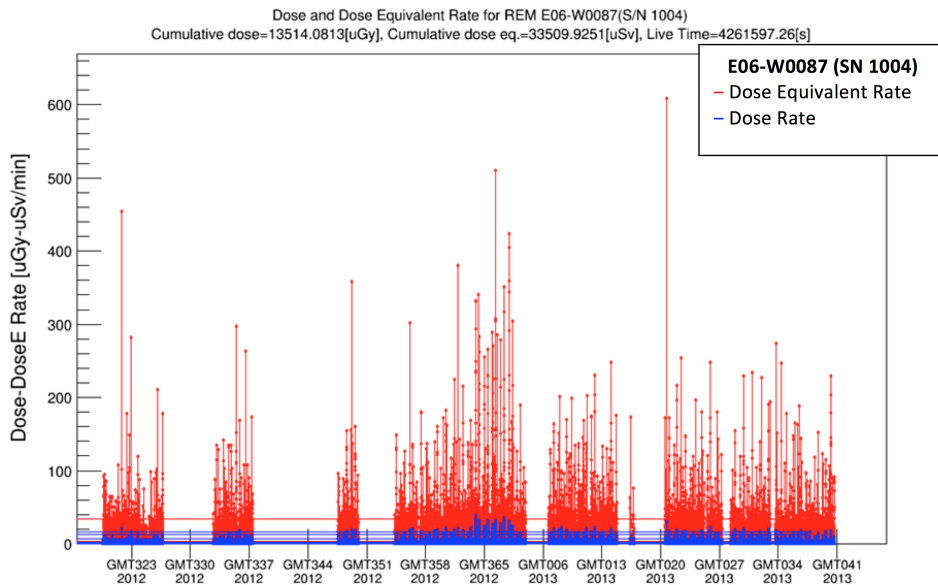


Figure 6: SN 1004 dose rate and dose equivalent rate as a function of time.

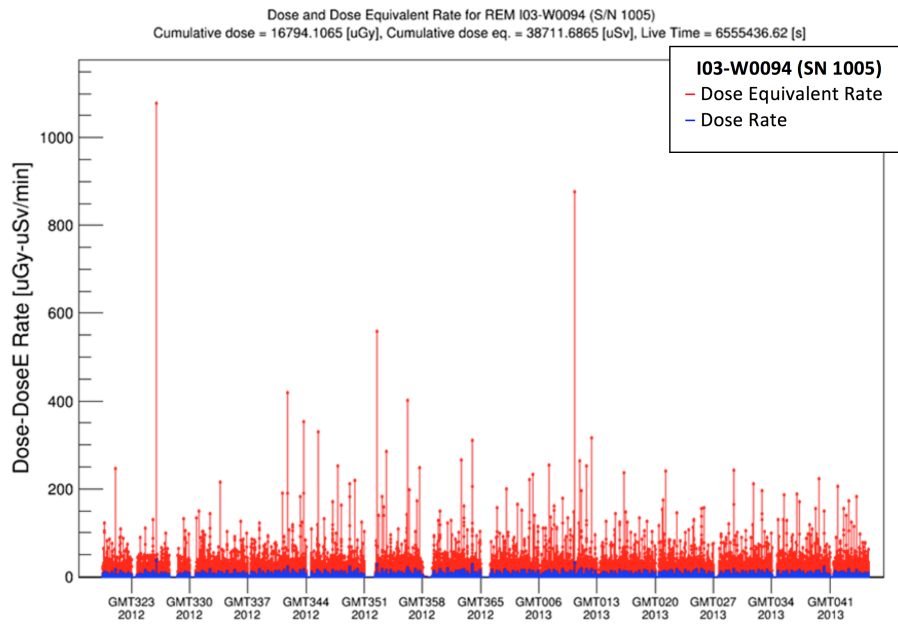


Figure 7: SN 1005 dose rate and dose equivalent rate as a function of time.

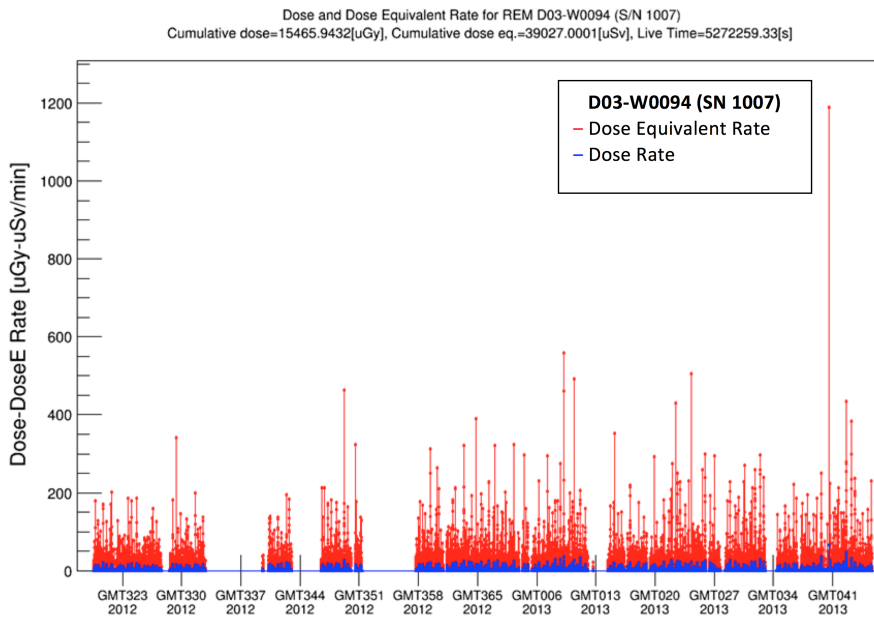


Figure 8: SN 1007 dose rate and dose equivalent rate as a function of time.

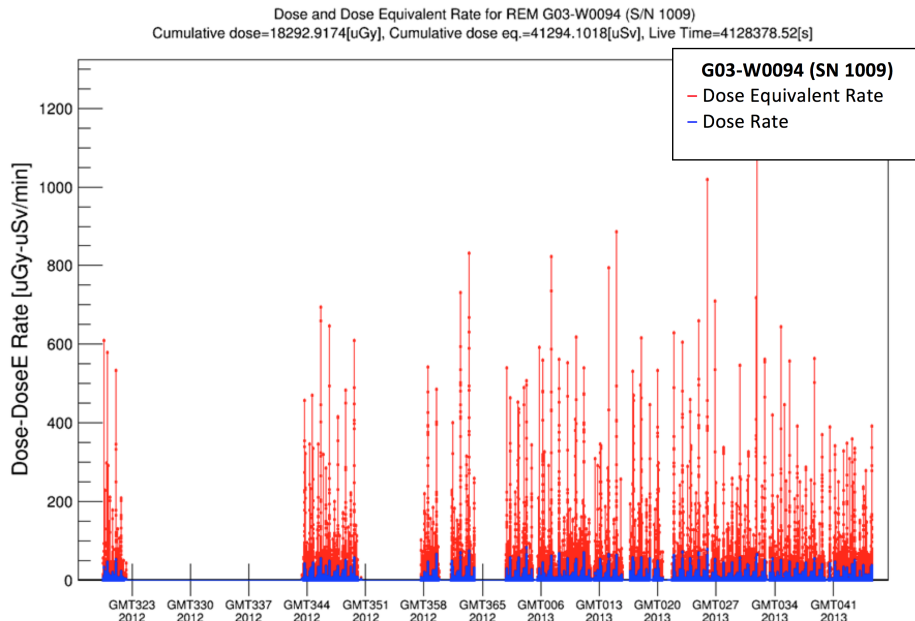


Figure 9: SN 1009 dose rate and dose equivalent rate as a function of time.

Artifacts present in the dose rate plot for ISS REM SN 1004 (Chip ID E06-W0087) are related to the way in which the analysis software plots the data points for a very small number of data points with invalid time stamps. Such data points are isolated to the metadata (start time, acquisition parameters, etc.) associated with a small subset of frames for ISS REM SN1004 on GMT 2013/035 through GMT 2013/038. The corrupted metadata may be due to instrument resets or other hardware issues. Work is in progress to identify the root cause of these rare data points and whether this issue is related to SN1004 unit failure.

The dose rate and dose equivalent rate for all units is generally consistent across ISS REM devices, as can be seen in the comparison plots for GMT 2013/029 in figures 10 and 11. Location, vehicle shielding, and orientation may contribute to variance in dose rates between devices. Spikes in dose equivalent values can be traced back to high LET tracks similar to that shown in the inset of the per-frame dose rate plot for ISS REM SN 1003 in figure 5. The inset contains a frame of data with a high LET ($250 \text{ keV}/\mu\text{m}$) track, and the pattern of energy deposition in the pixel matrix resulting from the primary particle track, as well as that from the secondary electrons scattered by the primary particle, is visible.

The comparison with IV-TEPC data is plotted on a shorter time scale so that variations in dose and dose equivalent rates can be more clearly seen. In these comparisons, ISS REM dose rates are averaged over a 60-second window corresponding to IV-TEPC data timestamps. The latter is done to mimic the measurement method used by IV-TEPC and to provide a consistent comparison to IV-TEPC dose rates.

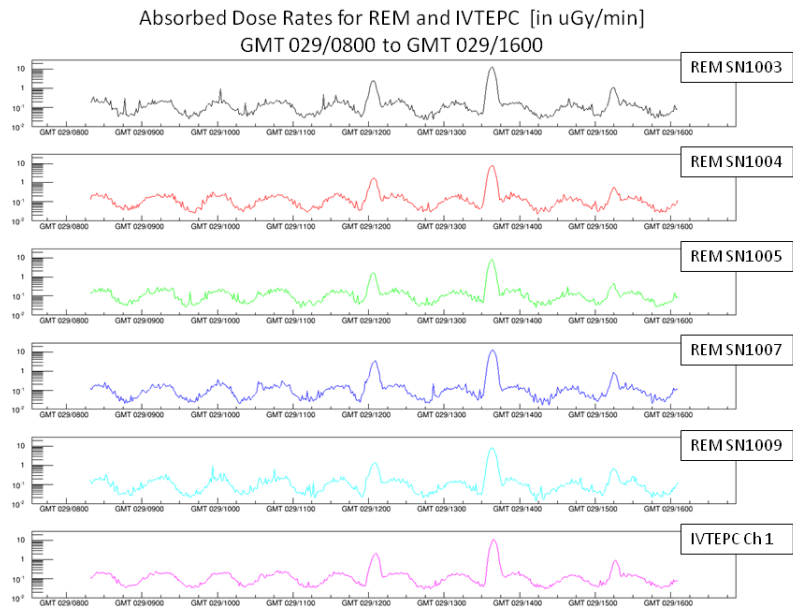


Figure 10: Comparison of dose rates for REM and IV-TEPC detectors aboard ISS

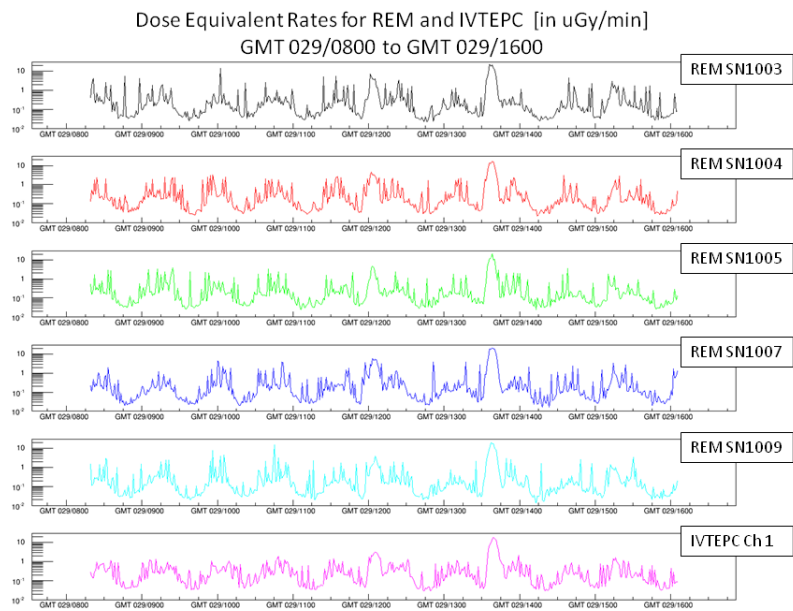


Figure 11: Comparison of dose equivalent rates for REM and IV-TEPC detectors aboard ISS

Percent Daily Coverage						
	SN1003	SN1004	SN1005	SN1007	SN1009	IVTEPC Ch1
GMT024	100.0%	100.0%	99.6%	100.0%	100.0%	100.0%
GMT025	100.0%	79.2%	100.0%	100.0%	100.0%	100.0%
GMT026	100.0%	100.0%	100.0%	66.5%	67.5%	100.0%
GMT027	86.2%	38.4%	38.5%	64.2%	86.0%	100.0%
GMT028	100.0%	59.3%	100.0%	62.8%	100.0%	100.0%

Trapped Radiation Daily Dose [μGy]						
	SN1003	SN1004	SN1005	SN1007	SN1009	IVTEPC Ch1
GMT024	169.9	127.4	85.4	151.8	348.0	158.4
GMT025	244.8	199.8	119.4	220.1	495.2	237.3
GMT026	145.1	120.3	72.7	155.6	296.6	145.8
GMT027	121.4	20.7	52.8	30.4	294.5	192.9
GMT028	179.2	136.5	85.5	157.5	237.6	162.4

GCR Daily Dose [μGy]						
	SN1003	SN1004	SN1005	SN1007	SN1009	IVTEPC Ch1
GMT024	143.6	146.7	137.4	126.3	129.2	137.5
GMT025	139.7	106.5	135.0	122.3	129.3	134.0
GMT026	148.0	144.2	137.8	73.5	79.7	133.6
GMT027	124.3	60.6	43.8	86.3	106.9	132.4
GMT028	142.3	78.6	137.8	72.2	129.0	136.4

Figure 12: Percent coverage tables. Daily coverage less than 95% is shown in light gray.

Within this 8-hour time frame, the low level variation of dose and dose equivalent rate associated with high latitude ISS passes can be seen, along with the peaks associated with SAA transits. The ISS REM data correlates well with IV-TEPC data, and it is clear from the data that the ISS REM hardware is capable of handling both the dose rates in the high latitude regions of the vehicle orbit and the dose rates through the SAA.

In addition to the plots in figures 10 and 11, tabular data for daily dose comparisons to IV-TEPC is provided in figures 12 and 13 along with the related instrument live time for comparison of trapped and GCR components. Text has been made lighter in color to differentiate entries in the dose tables which correspond to daily coverage for the detector of less than 95%. Variations in the trapped doses are expected due to the dependence of trapped radiation dose on location inside the vehicle.

A second set of tabular data is shown in figure 14 which has been scaled to non-SAA live time (per day) in order to show the consistency of dose and dose equivalent

for the GCR component across ISS REM units. The scaling is done for each ISS REM unit relative to IV-TEPC detector live time for the same regions, and using the same SAA/non-SAA separation as used for IV-TEPC. See Appendix D for a complete set of data tables for the same time period.

Percent Daily Coverage GCR (relative to IVTEPC)						
	SN1003	SN1004	SN1005	SN1007	SN1009	IVTEPC Ch1
GMT024	100.00%	100.00%	99.57%	100.00%	100.00%	100.00%
GMT025	100.00%	77.99%	100.00%	100.00%	100.00%	100.00%
GMT026	100.00%	100.00%	100.00%	64.77%	65.86%	100.00%
GMT027	87.20%	40.03%	37.45%	66.81%	87.12%	100.00%
GMT028	100.00%	58.01%	100.00%	61.62%	100.00%	100.00%

Figure 13: Percent coverage of GCR relative to IV-TEPC

Scaled Daily GCR Dose [μGy]						
	SN1003	SN1004	SN1005	SN1007	SN1009	IVTEPC Ch1
GMT024	143.6	146.7	138.0	126.3	129.2	137.5
GMT025	139.7	136.6	135.0	122.3	129.3	134.0
GMT026	148.0	144.2	137.8	113.5	121.0	133.6
GMT027	142.5	151.4	116.9	129.2	122.7	132.4
GMT028	142.3	135.4	137.8	117.2	129.0	136.4

Scaled Daily GCR Dose Equivalent [μSv]						
	SN1003	SN1004	SN1005	SN1007	SN1009	IVTEPC Ch1
GMT024	430.5	468.1	407.5	486.9	443.8	448.8
GMT025	399.8	462.5	387.0	426.5	440.2	417.7
GMT026	483.9	485.1	404.5	402.6	422.3	410.0
GMT027	456.0	559.2	350.8	518.9	461.5	413.5
GMT028	405.4	393.4	401.7	384.3	467.2	432.4

Figure 14: Dose and Dose equivalent scaled relative to percent daily coverage.

4.2 Orbital Dose Rate Maps

Dose maps of ISS REM data versus ISS latitude and longitude (figures 15 through 19) show variations that agree with total dose, total dose equivalent, and effective quality factors for the time-dependent and tabular data for each of the respective units. ISS REM units which show quality factors closer to that expected from protons also show higher dose rates during SAA transits.

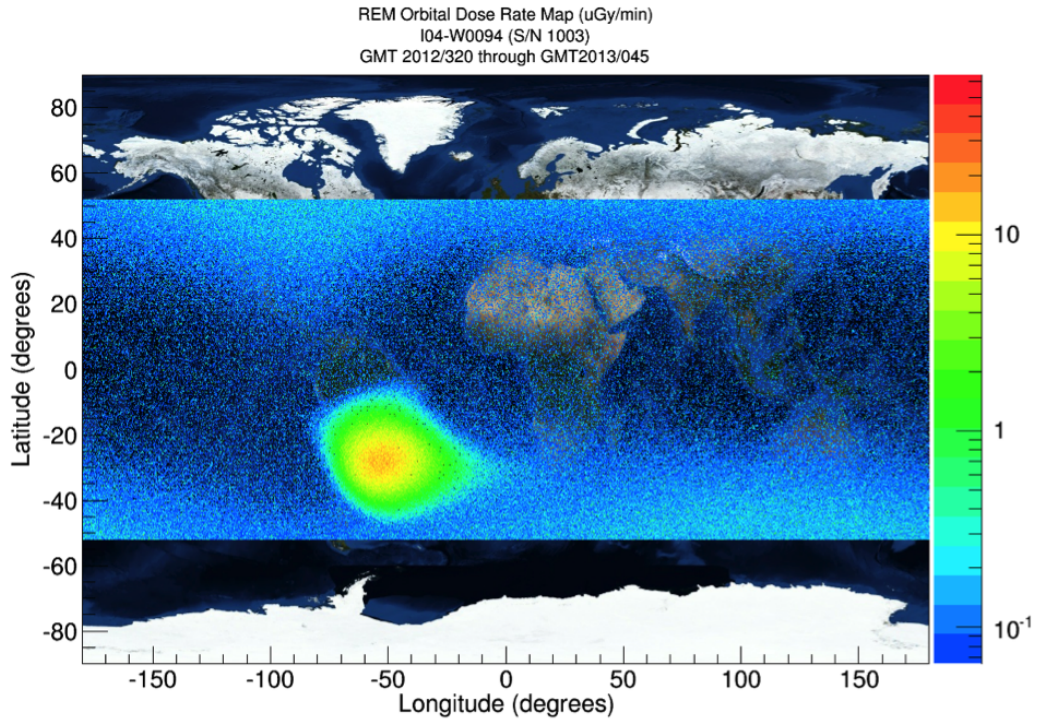


Figure 15: Dose rate map for ISS REM unit SN1003.

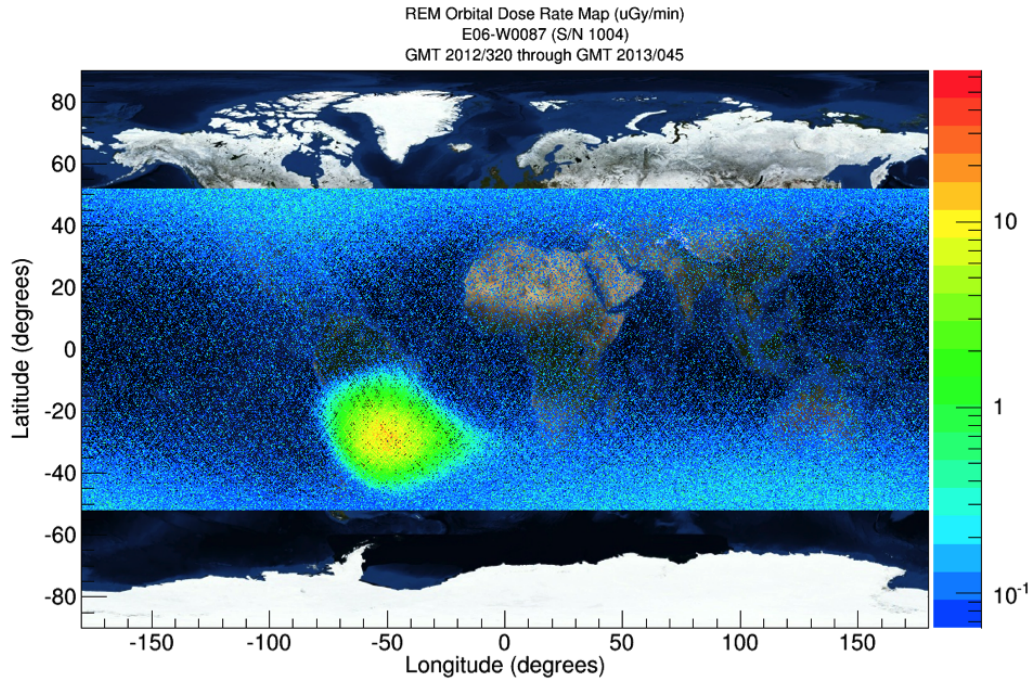


Figure 16: Dose rate map for ISS REM unit SN1004.

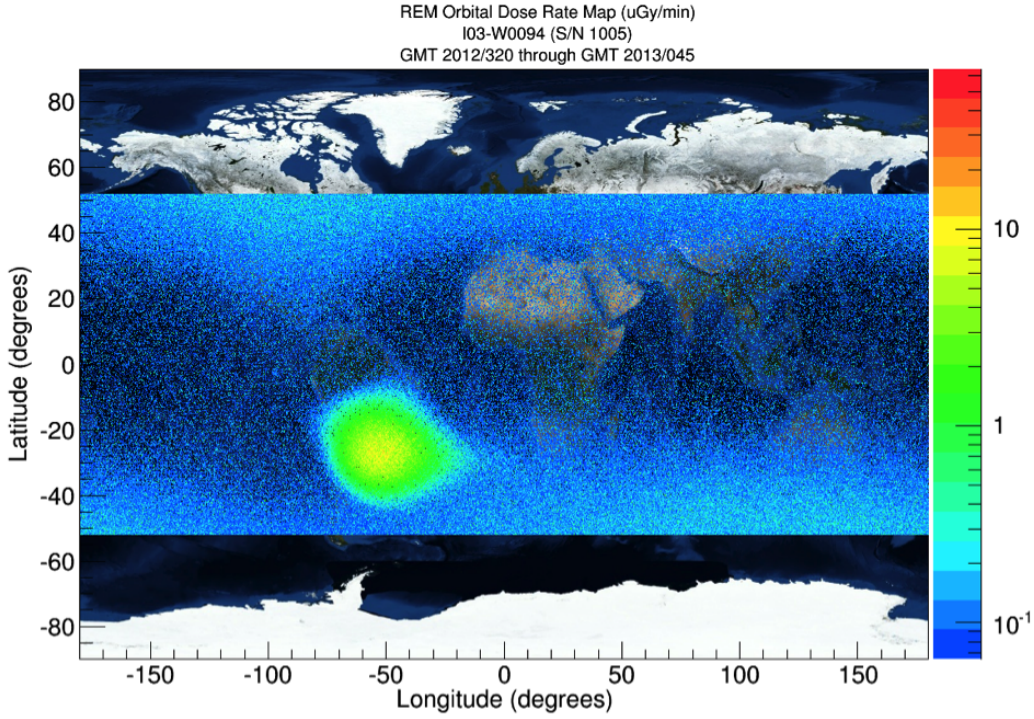


Figure 17: Dose rate map for ISS REM unit SN1005.

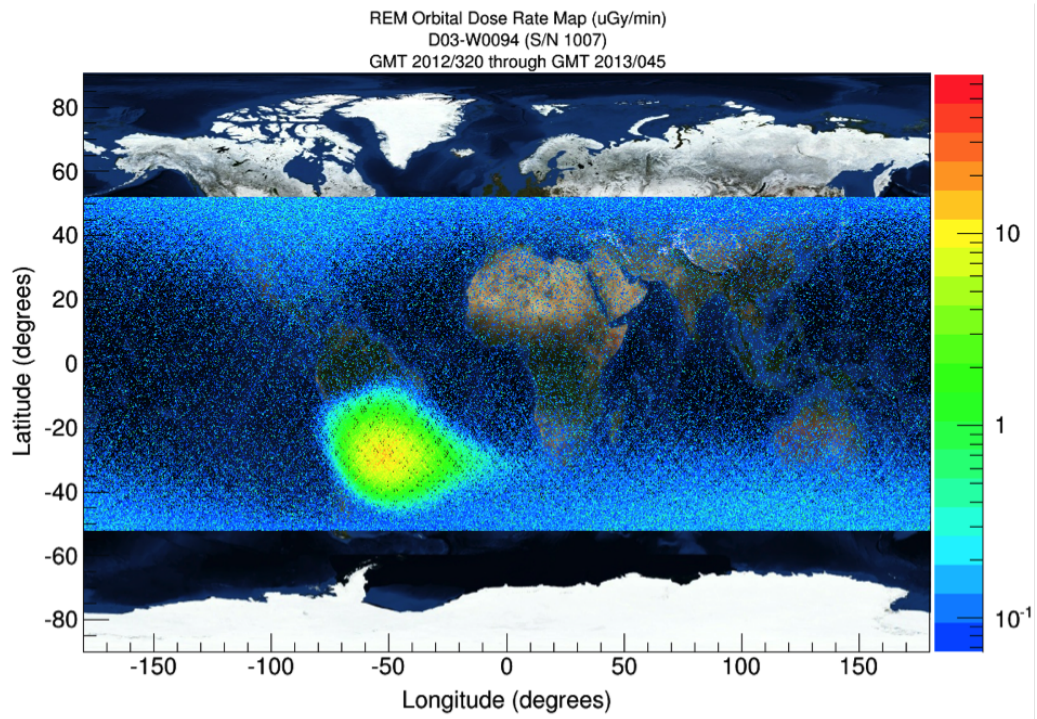


Figure 18: Dose rate map for ISS REM unit SN1007.

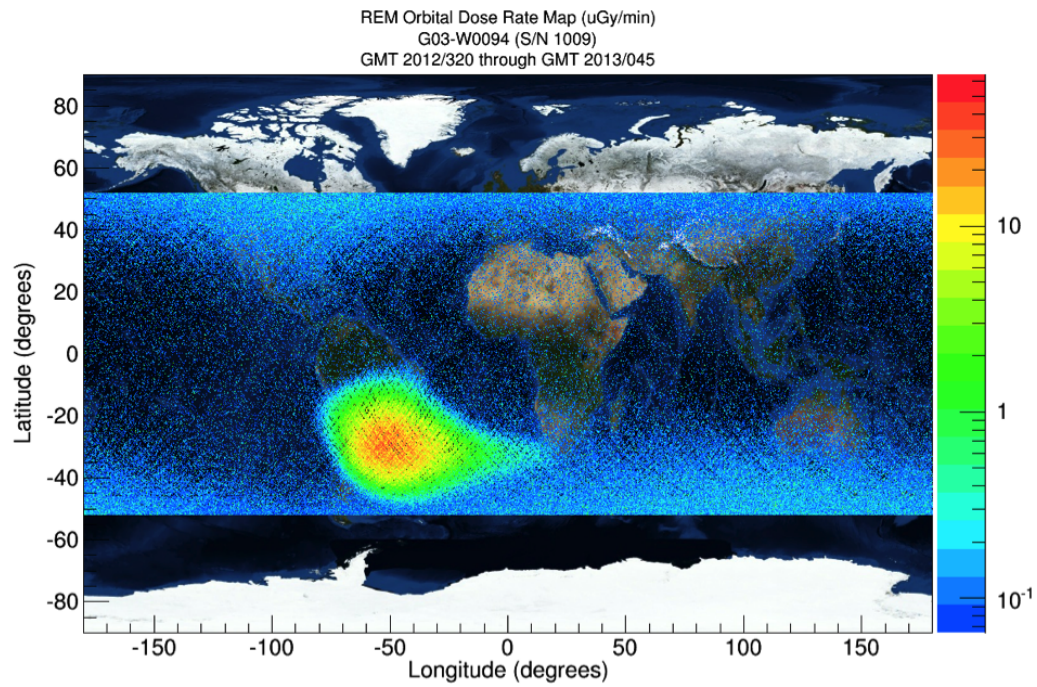


Figure 19: Dose rate map for ISS REM unit SN1009.

4.3 Linear Energy Transfer Distributions by Device

After the unit specific calibration is applied, the ISS REM hardware provides energy deposition in each pixel. The resulting cluster patterns allow for extraction of both energy and track angle information for each particle track. Using this information, the linear energy transfer (LET) can be calculated on a per-track basis. Figures 20, 21, and 22 show the per-track LET distribution during the entire analysis period.

Further characterization of the LET distribution based on orbital location can be carried out, and a simple separation of the total LET distribution into SAA and non-SAA components is shown below.³

The variations between devices for LET above $1 \text{ keV}/\mu\text{m}$ are consistent relative to one another for non-SAA orbital locations, while the LET distributions in the SAA regions show more pronounced variations between the different devices. Variations in shielding mass distribution around the different ISS REM device locations may account for the LET variations between devices within the non-SAA distributions. In addition to the mass distribution differences, the variations below $1 \text{ keV}/\mu\text{m}$ could be related to variations in LEO electron component and subsequent penetration of such electrons through the vehicle mass and/or secondary particle production at the ISS REM deploy locations.

For reference, minimum ionization stopping powers for protons, alphas, and carbon are approximately $0.4 \text{ keV}/\mu\text{m}$, $1.6 \text{ keV}/\mu\text{m}$, and $14.2 \text{ keV}/\mu\text{m}$ respectively. See Appendix C for plots of LET spectra by device with the associated SAA locations. Appendix C also contains the raw (un-normalized) LET distributions.

In comparing the LET distributions for SAA and non-SAA components, it was observed that the LET distribution in the SAA had a larger peak near $14 \text{ keV}/\mu\text{m}$ than did the non-SAA component. This observation was contrary to expected results.

Under the assumption that the peak in the LET spectrum near $14 \text{ keV}/\mu\text{m}$ is a result of minimum ionizing carbon ions prevalent in the GCR, the SAA component of the LET spectrum around $14 \text{ keV}/\mu\text{m}$ is expected to be equal to or less than that in the non-SAA LET spectrum. The increase in SAA component of the LET spectrum near $14 \text{ keV}/\mu\text{m}$ was found to be related to protons stopping in the ISS REM sensor layer. The related investigation is discussed in more detail in the next section.

³The SAA separation algorithms for the ISS REM data are still in development, and the data shown for such separations utilizes the variation in acquisition time to identify the South Atlantic Anomaly. This acquisition-time based method is not optimal for determination of the SAA. Since acquisition time is related to flux, using such a method introduces a device-specific dependence on the definition of the SAA location resulting from detector orientation and local detector shielding variations. In addition, such a method assumes there are no Solar Particle Events or geomagnetic storm periods during the analysis period that would affect local particle flux.

Despite these drawbacks, and due to the relative quiescence of the LEO radiation environment during the analysis period, the use of this method of SAA definition in this specific application does allow a rough comparison of LET distributions for SAA and non-SAA locations. The comparisons for total, SAA, and non-SAA LET distributions are shown for the five ISS REM units on orbit. These distributions are in terms of particles per second and are normalized to acquisition time totals for each device and location to allow comparison between devices. As expected, particle count rates are higher in the SAA locations than in non-SAA areas.

LET Distribution

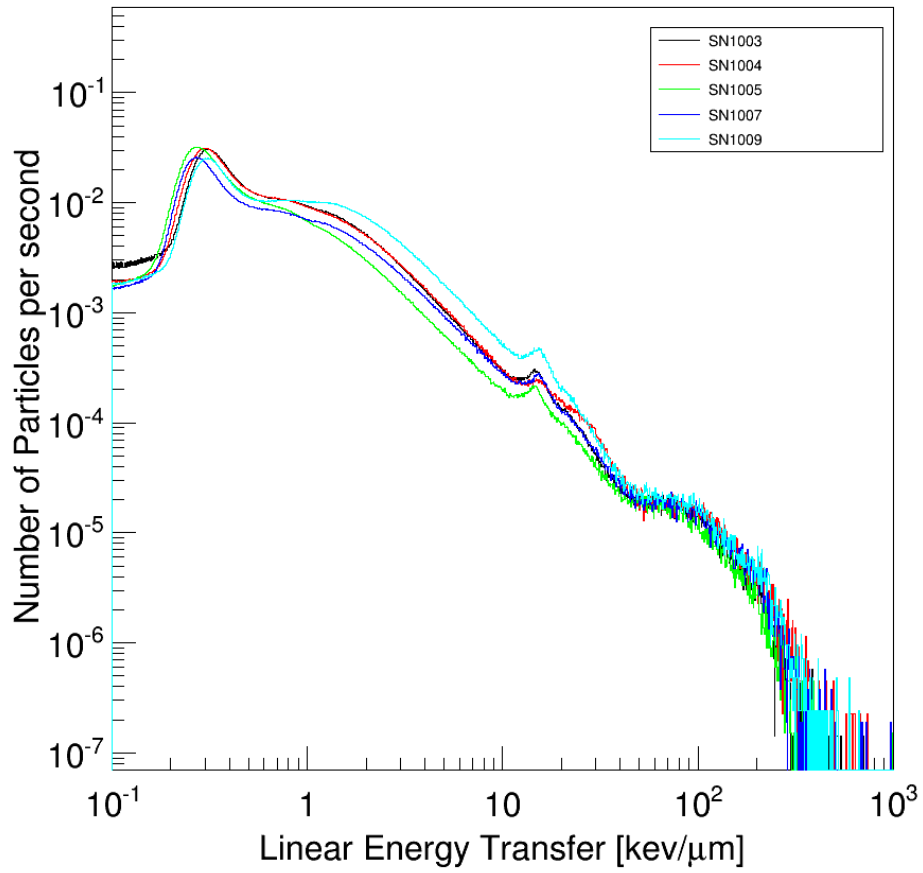


Figure 20: LET spectra for all 5 REM units

LET Distribution (SAA only)

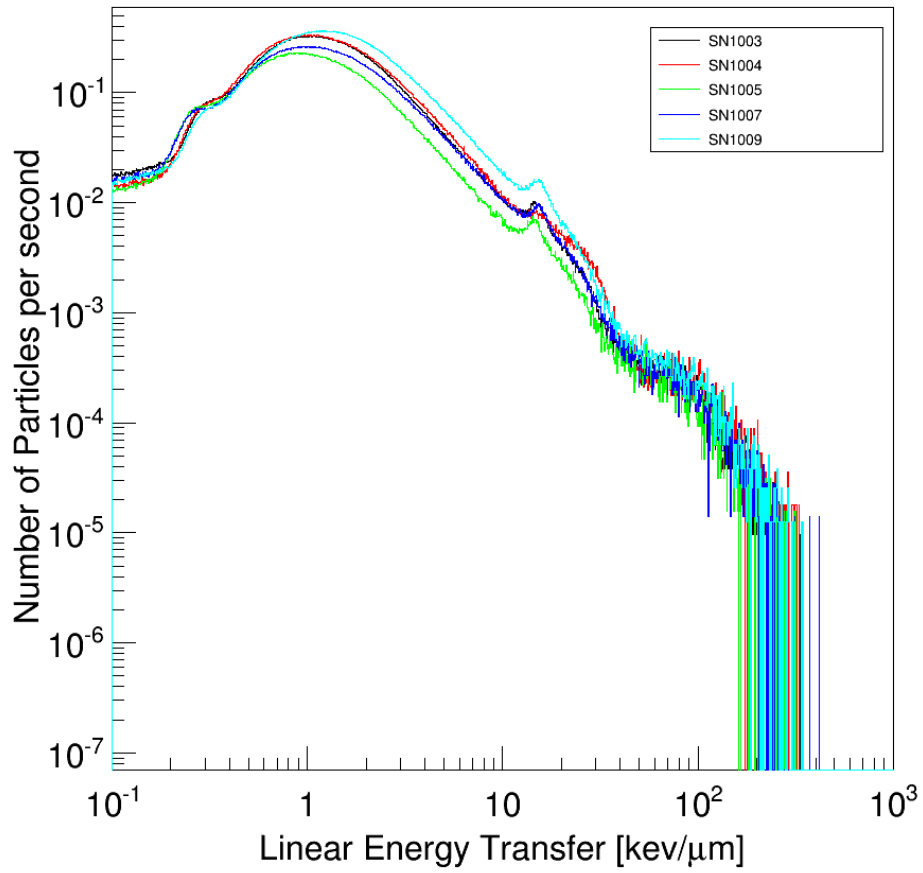


Figure 21: LET spectra for all 5 REM units in the South Atlantic Anomaly

LET Distribution (Not including SAA)

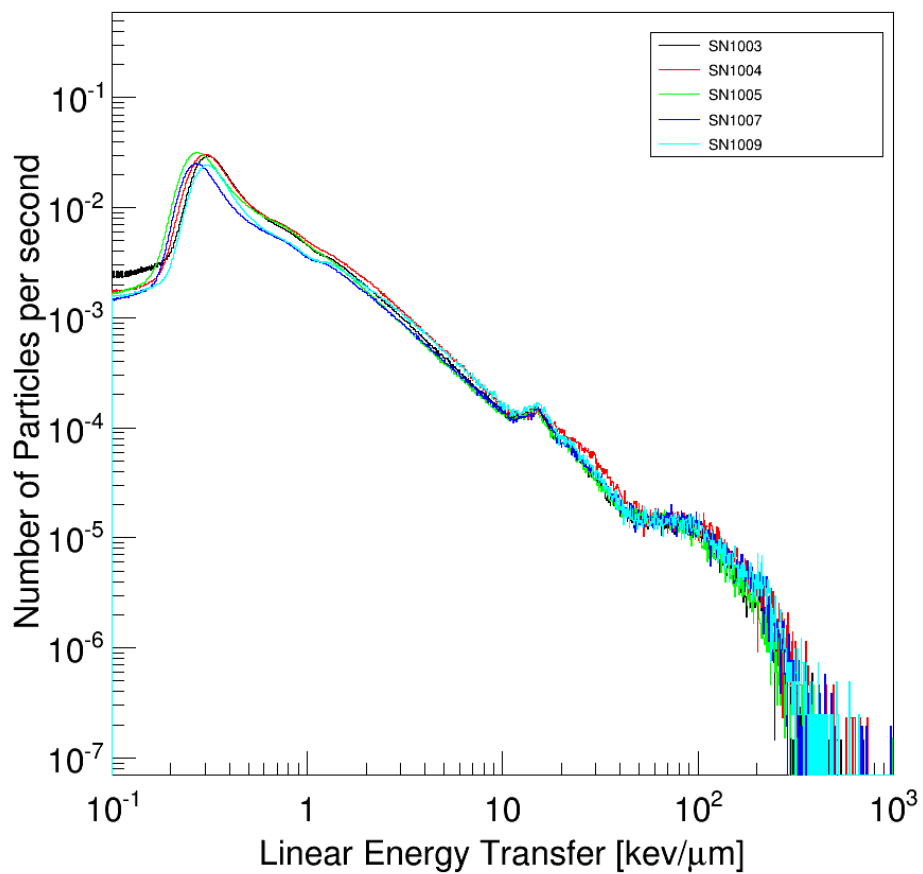


Figure 22: LET spectra for all 5 REM units outside of the South Atlantic Anomaly

5 Ongoing Research and Development

Spaceflight applications of the Timepix technology are being developed through the Advanced Exploration Systems (AES) Project with hardware built to fly on the Orion Exploration Test Flight 1 (EFT-1) mission. The AES Battery-operated Independent Radiation Detector (BIRD) is designed to operate for the duration of the EFT-1 mission and save unprocessed Timepix data for post-flight analysis. The BIRD hardware is designed to operate independently of Orion systems and to utilize battery power for the entire mission duration. This project provides both a demonstration of the applicability of the Timepix technology for use on exploration missions, as well as the collection of radiation environment data in preparation for manned flights to similar orbits.

The nature of the data provided by the Timepix device allows the calculation of track angles relative to the detector surface normal as well as in the plane of the detector surface. The angular distribution of trapped particles is known to be different than that of GCR particles, and this difference is discernible in the angular distributions generated using ISS REM data. Significant progress has been made in increasing the angular resolution; however, issues relating to determining exact detector location and orientation within the vehicle are still being addressed.

The possibility of neutron detection also exists using the Timepix detectors. ISS REM SN 1009 incorporates a layer of neutron conversion material (^6LiF) on one half of the detector face. While the effectiveness of this method of neutron detection is under investigation, thus far, the preliminary estimation of neutron flux is consistent with models for the LEO environment.

The ISS REM project is providing data for use in development of techniques to separate heavy ion tracks from proton and alpha particle tracks in all portions of the ISS orbit, as well as techniques to separate particle interaction tracks. The ultimate goal of this research is to be able to characterize the radiation field within a vehicle based on data from Timepix pixel detectors. Such data shows promise in being able to categorize both the charge and the velocity of particles traversing the silicon detector. This investigation is ongoing in collaboration with the University of Houston Physics Department, IEAP, and the Medipix Collaboration.

Preliminary analysis performed on the ISS REM data shows high LET tracks are more prevalent in higher latitude regions and within the SAA. The plots below show orbital locations of particle tracks with an associated LET of greater than $50 \text{ keV}/\mu\text{m}$ for GMT 2013/043 to GMT 2013/045. Limiting selection of data for plots over the same time period using an alternate selection criteria that is LET independent yields similar results, as can be seen in the final plot.⁴

While it is clear that there are genuine GCR relativistic heavy ions present in the SAA, it is also clear from these plots that a significant fraction of the high-LET events in the SAA are low energy target-fragments that result from nuclear colli-

⁴The alternate selection criteria used in the final plot is a cut on the data to limit to those tracks that have more than one local maximum in the cluster energy deposition pattern and also deposit more than 1.5 MeV in a single pixel. The limitation to clusters with one local maximum excludes interaction tracks and overlapping particle tracks, while the cut on single pixel energy deposition excludes lower energy particle tracks.

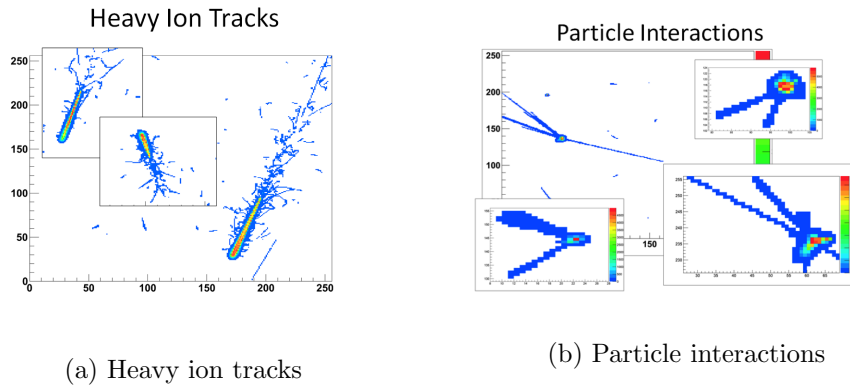


Figure 23: Various tracks from on-orbit data showing signatures of heavy ion traversal (a) and particle interactions (b) within the detector. Note the prevalence of delta rays surrounding the core track structure in (a).

sions of the incident radiation (mostly trapped protons) with the detector materials themselves, both within the sensor layer and immediately external to it. Algorithms are in development to distinguish these background interaction events so that they can be handled properly in the ensuing dose and dose-equivalent estimates.

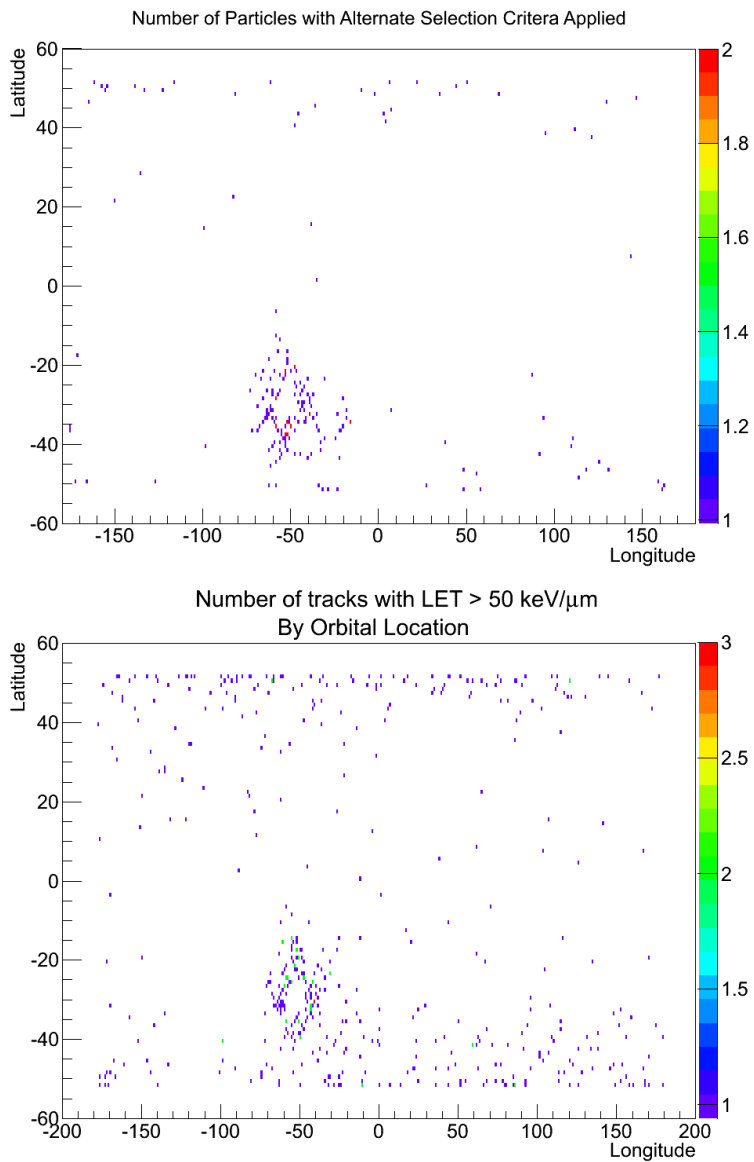


Figure 24: These images show two methods of isolating heavy ion tracks in ISS REM data with the results plotted according to orbital location.

5.1 Stopping Ion Identification

As mentioned in the LET distribution discussion, comparison of the SAA and non-SAA LET distributions revealed an unexpected difference between those two LET spectra near $14 \text{ keV}/\mu\text{m}$. Investigation into the matter has revealed that the issue is related to ions, primarily protons, stopping within the $300 \mu\text{m}$ silicon detector layer.

A simulation of the energy loss estimated from SRIM⁵ coupled to path length variation for protons with energies between 1 and 50 MeV traversing a $300 \mu\text{m}$ thick planar silicon sensor was performed using the same principles for angle identification as used in the ISS REM analysis algorithms. Simulation results show very clearly that the LET peak near $14 \text{ keV}/\mu\text{m}$ results from the manner in which the angle and path length are calculated for these stopping ions.

The results of the simulation are shown in figure 25 along with the relevant data for comparison. In the simulation, counts are arbitrary and serve only to show the relative contribution. The simulated proton LET distribution contains a component attributable to the stopping protons, visible as the triangular region between 12 and 21 $\text{keV}/\mu\text{m}$ in the plot. Comparison of on-orbit data to the simulation output illustrates that the simulated stopping proton distribution is well correlated with the feature seen in the on-orbit LET versus energy plot for the ISS REM particle track data. It was also found that a minor reduction in the range for simulated protons further increased the correlation between simulation results and on-orbit data in the tail of this region. This has led to an ongoing investigation into sensor composition to identify impacts of variations in sensor composition on parameters relating to particle identification.

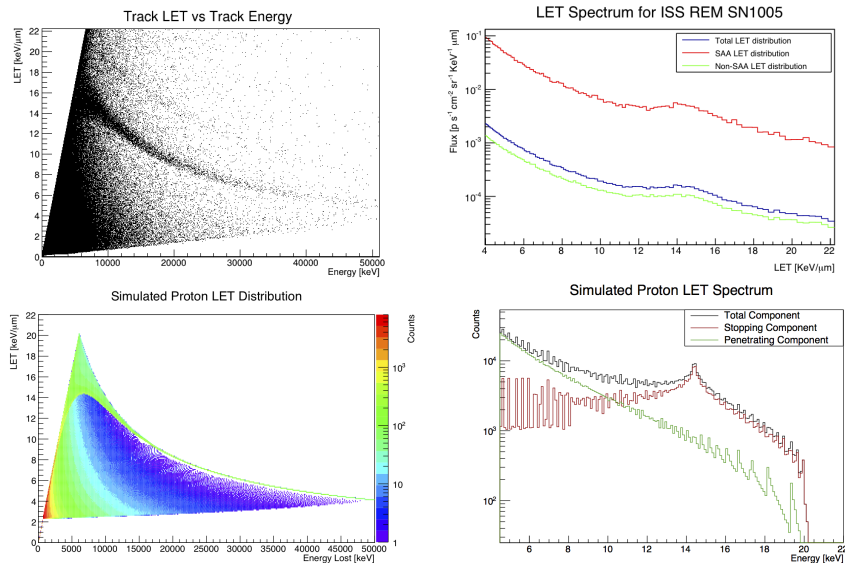


Figure 25: Measured and simulated energy distribution of protons in the Timepix detector

⁵<http://www.srim.org>

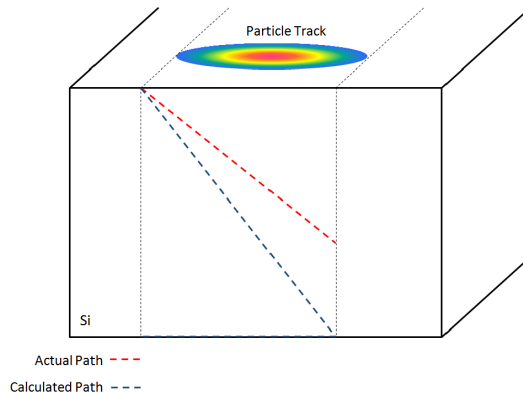


Figure 26: Visualization of the error introduced to path length by misidentification of stopping protons

The prevalence of the stopping ions poses several issues which make it necessary to identify such ions within the data sets. The calculation of Linear Energy Transfer (LET) is based upon a supposition of full traversal of the ion through the silicon detector and provides the average energy lost along the path of the ion. The ion path length is calculated from the projection of the three-dimensional ionization track into the two-dimensional charge collection plane of the detector. If the ion ranges out and stops prior to completing the traversal of the silicon detector layer, the identified angle of incidence is smaller, and the calculated path length is longer, than that of the actual track. This results in an incorrect LET estimate for the ion.

In addition, due to the increase in the rate of energy deposition as the stopping ion loses energy during its traversal of the silicon layer, the concept of an average energy loss, such as the calculated LET for stopping ions, becomes less useful for the determination of a quality factor to apply toward estimates of biological effectiveness.

The problem is not intractable, however, and analysis of ISS REM data on a per-track basis indicates identification of stopping ions is feasible. Such identification is currently being tested within the data analysis algorithms currently under development.

6 Conclusion

Initial analysis of the ISS REM on-orbit data has shown the devices perform at or beyond expectations. Calculated ISS REM dose rates are similar to those from existing ISS radiation hardware, and the ISS REM units have demonstrated the capability to measure the incident particle flux from both Galactic Cosmic Rays and ions trapped within the Van Allen belts.

Research and development efforts have provided a toolset to analyze on-orbit ISS REM data and provide per-track incidence angle and Linear Energy Transfer estimates with an increasing capability to identify heavy ion tracks and particle interactions. Such efforts are also providing data on Timpix-based neutron detection as well as on stopping ion identification and its relation to LET spectra, with the ultimate goal of characterizing the ionizing radiation field within a vehicle based on individual particle charge and velocity.

Appendix A

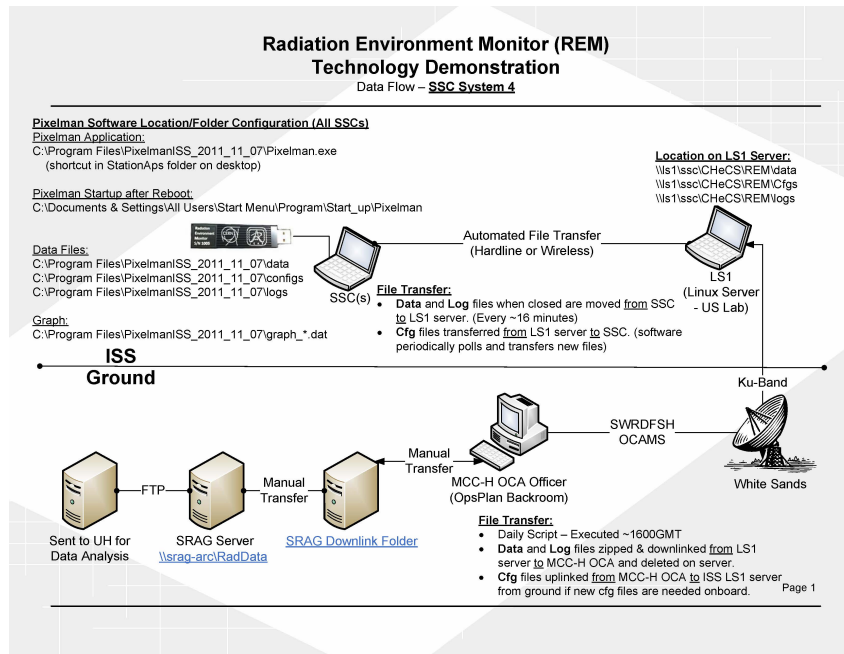
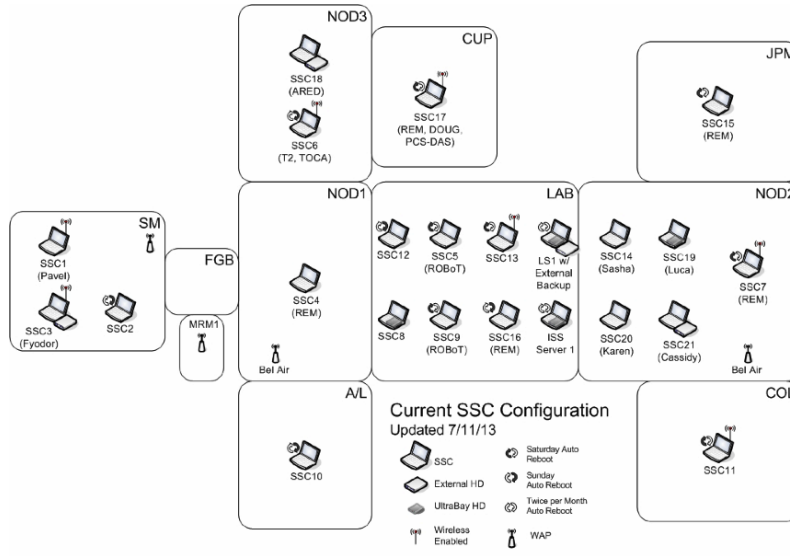
ISS REM Uplink Log

GMT 2012/291 (October 17, 2012)	Uplinked config files for all dosimeters. <u>S/N 1009 Config file missing from original SSC Pixelman software load.</u>
GMT 2012/297 (October 23, 2012)	<p>File uplink with the reduced <u>occupancy parameters.</u></p> <p>G03-W0094: Debug message output level reduced to level2 to minimize log file size StartAcqOnStartup is set to 'true'</p> <p>All units: PixCountParam1=655.0 PixCountParam2=1965.0 PixCountParam3=3275.0 LetB=2.2 LetLmax=100</p>
GMT 2012/299 (October 25, 2012)	<p>The factors are the parameters that execute the acquisition time change, while the Param entries set the values for comparison of each frame. The change to the dosimeter.ini file will <u>set an upper limit on log file size and control the log files on the SSCs so they don't get unmanageable in size.</u></p> <p>The changes incorporated for the files in the GMT299 uplink are as follows:</p> <p>dosimeter.ini file: LogFileSizeLimit=15000000</p> <p>All unit individual .ini files: PixCountParam1=655.0 PixCountParam2=1966.0 PixCountParam3=3276.0</p> <p>PixVolumeParam1=3.869e6 PixVolumeParam2=1.935e7 PixVolumeParam3=3.869e7</p> <p>FactorPC1=0.009995 FactorPC2=1 FactorPC3=0.029998</p> <p>FactorPV1=4.99884e-3 FactorPV2=1 FactorPV3=0.049988</p>
GMT 2012/307 (November 02, 2012)	<p>Dosimeter .ini files uplinked to <u>disable the XYGrid function in the framerate algorithm.</u> Currently we have a few high occupancy frames within the SAA passes as a result of what seems to be areas with low occupancy in the preceding frame and this is verified by the logic ID in the dosimeter log file. Disabling the XYGrid function will eliminate this adjustment during SAA passes.</p> <p>The following changes were made to all dosimeter specific .ini files:</p> <p>XYPosEnable=false XYGridEnable=false</p>
GMT 2012/318 (November 13, 2012)	<p>After further analysis, the issue with periodic long frames during SAA passes was found to be due to an <u>adjustment parameter related to cluster count.</u> The intent of the adjustment was to increase acquisition time slightly when pixel count was not increasing but cluster count was decreasing over the same set of frames. The parameter has been changed so the acquisition time adjustment is much less dramatic.</p> <p>The change made to all 5 initialization files is as follows: The adjustment will now change a frame time of 0.80s to 0.89s (where the original setting would adjust 0.80s to 4.0s). Based on REM data from GMT312, the adjustment should maintain cluster separation in the SAA.</p> <p>FactorDP1=0.9 (from the original setting of 0.2)</p>

<p>GMT 2013/101 (April 11, 2013)</p>	<p>Uplinked calib *.txt, *.mcf, *.ini, and *.bpc files for S/N 1004 (E06-W0087) as part of the troubleshooting of this unit. The uplink of these configuration files was in preparation for the REM relocate activity currently scheduled for CDR on GMT 102/15:25 from SSC 13 to SSC 17. The REM team uplinked the specified configuration files for S/N 1004 unit to cover the possibility that the current onboard configuration files for this unit may be corrupted or the cause of the previous unit usb communication problems. (Flight Note F056356)</p> <p>calib_E06-W0087_a.txt calib_E06-W0087_b.txt calib_E06-W0087_c.txt calib_E06-W0087_letq.txt calib_E06-W0087_t.txt dosimeter_E06-W0087.ini USB_E06-W0087.bpc USB_E06-W0087.mcf</p>
<p>GMT 2013/194 (July 13, 2013)</p>	<p>Configuration files (*.mcf) uplinked for all units to increase bias voltage setting from 14.5 to 35. (Flight Note: F058047) .</p> <p>USB_DO3-W0094.mcf USB_E06-W0087.mcf USB_GO3-W0094.mcf USB_IO3-W0094.mcf USB_IO4-W0094.mcf</p> <p>All unit files: HV:14.5 to HV:35.0</p>

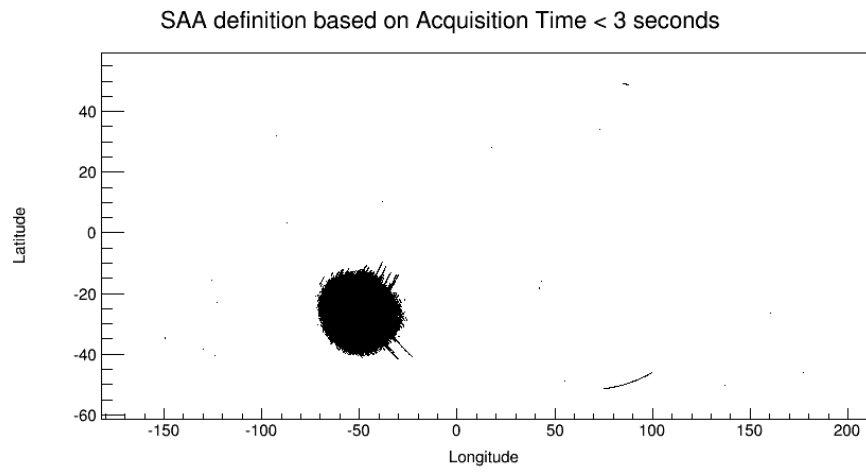
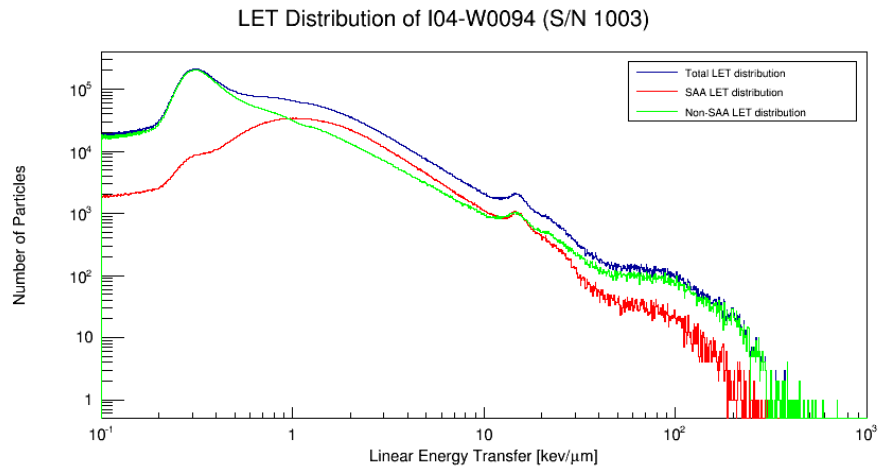
Appendix B

SSC Configuration and ISS REM Data Flow

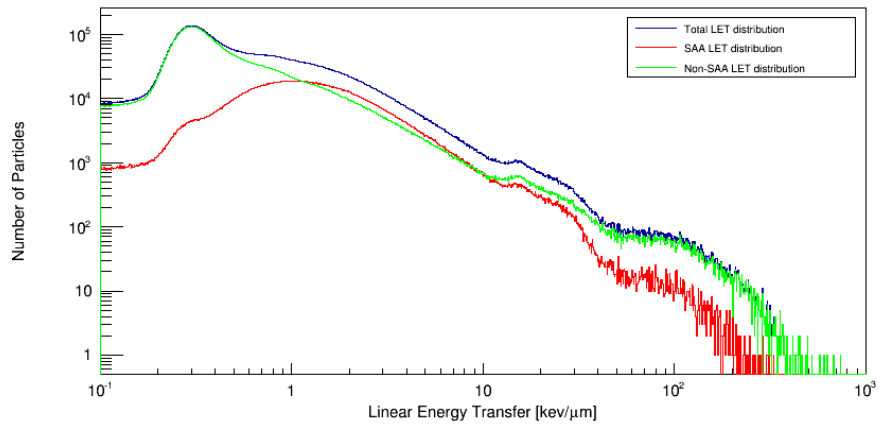


Appendix C

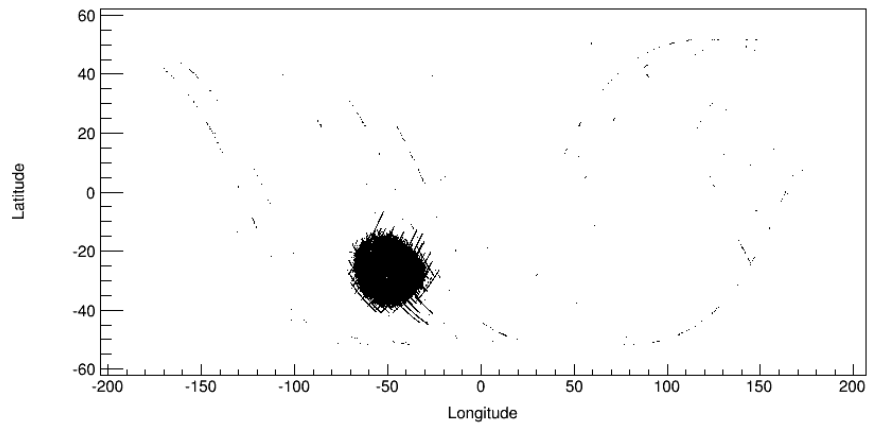
Raw LET Distributions



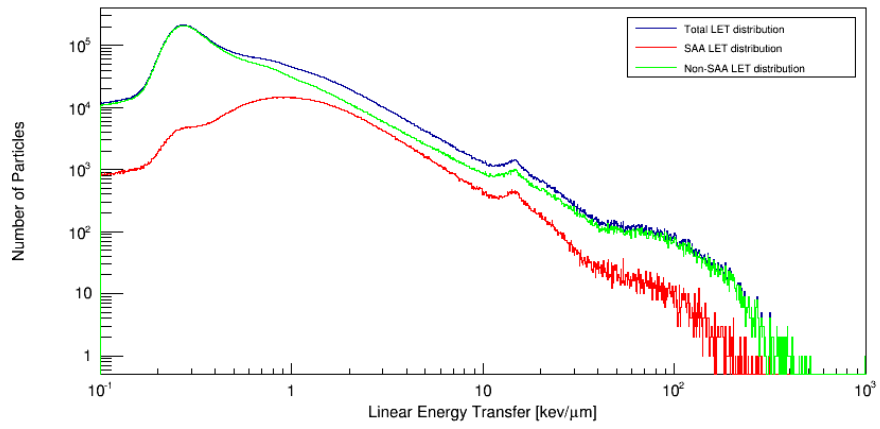
LET Distribution of E06-W0087 (S/N 1004)



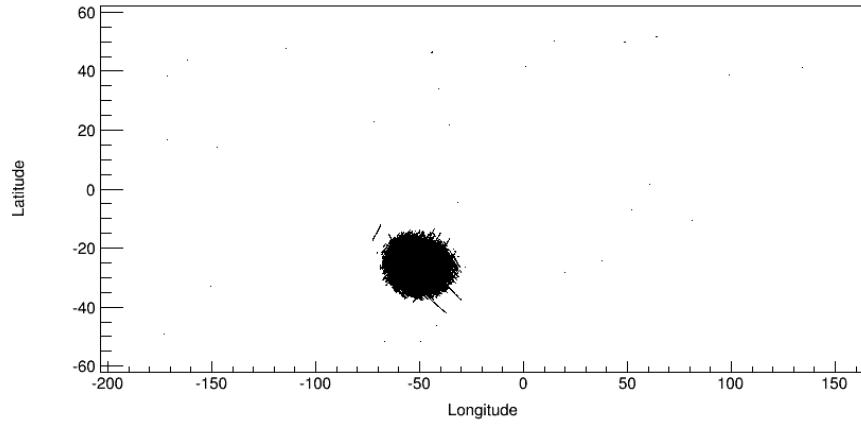
SAA definition based on Acquisition Time < 3 seconds



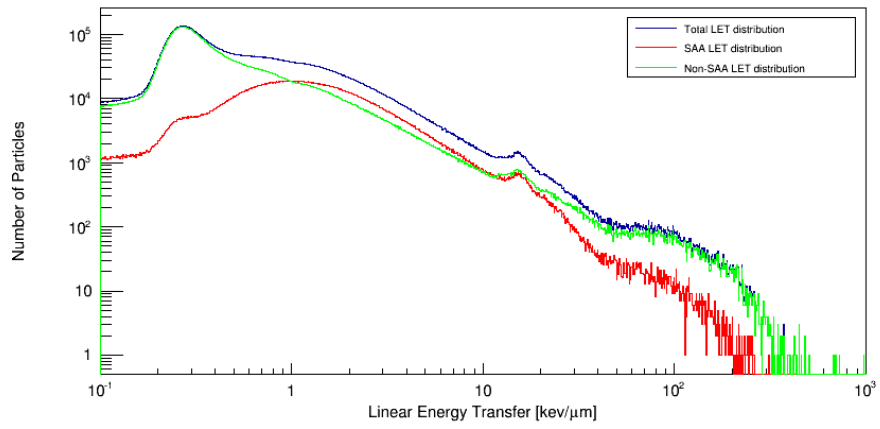
LET Distribution of I03-W0094 (S/N 1005)



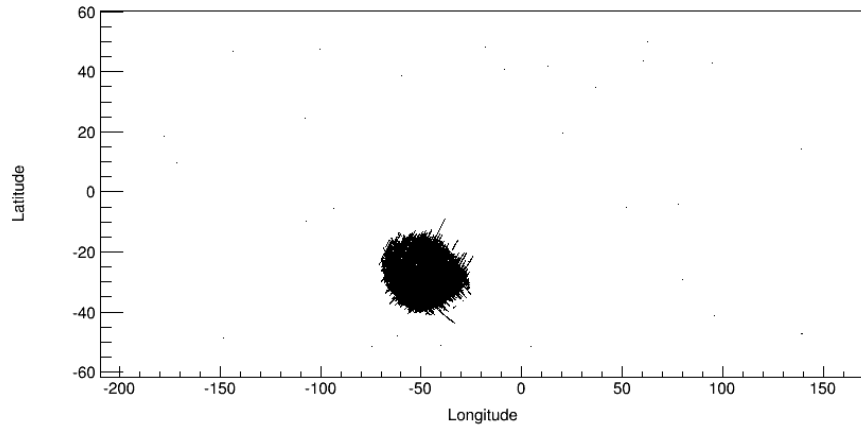
SAA definition based on Acquisition Time < 3 seconds



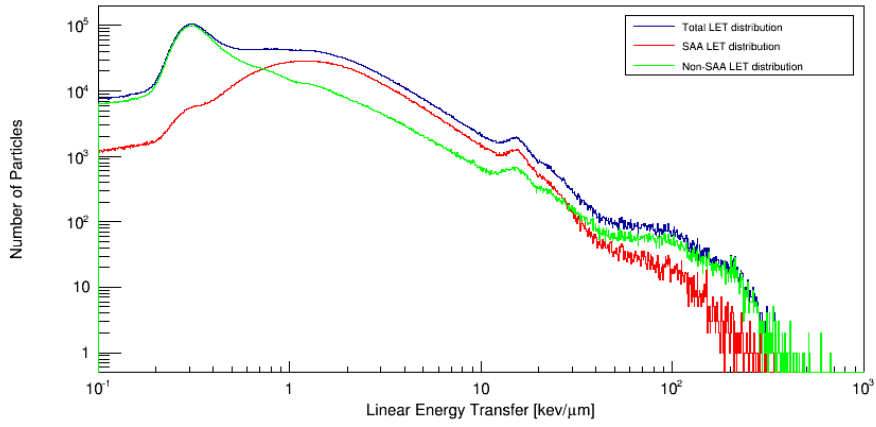
LET Distribution of D03-W0094 (S/N 1007)



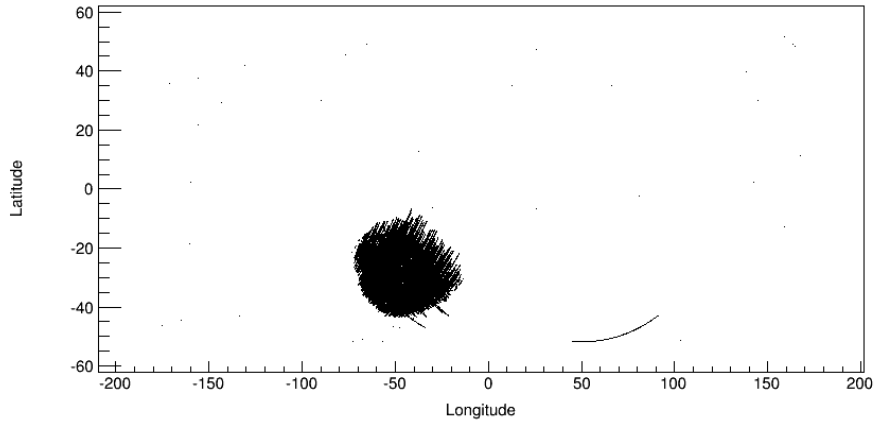
SAA definition based on Acquisition Time < 3 seconds



LET Distribution of G03-W0094 (S/N 1009)



SAA definition based on Acquisition Time < 3 seconds



Appendix D

Daily Dose Comparisons by Device with Quality Factor Comparison

Percent Daily Coverage						
	SN1003	SN1004	SN1005	SN1007	SN1009	IVTEPC Ch1
GMT024	100.0%	100.0%	99.6%	100.0%	100.0%	100.0%
GMT025	100.0%	79.2%	100.0%	100.0%	100.0%	100.0%
GMT026	100.0%	100.0%	100.0%	66.5%	67.5%	100.0%
GMT027	86.2%	38.4%	38.5%	64.2%	86.0%	100.0%
GMT028	100.0%	59.3%	100.0%	62.8%	100.0%	100.0%

Trapped Radiation Daily Dose [μGy]						
	SN1003	SN1004	SN1005	SN1007	SN1009	IVTEPC Ch1
GMT024	169.9	127.4	85.4	151.8	348.0	158.4
GMT025	244.8	199.8	119.4	220.1	495.2	237.3
GMT026	145.1	120.3	72.7	155.6	296.6	145.8
GMT027	121.4	20.7	52.8	30.4	294.5	192.9
GMT028	179.2	136.5	85.5	157.5	237.6	162.4
Trapped Radiation Daily Equivalent Dose [μSv]						
	SN1003	SN1004	SN1005	SN1007	SN1009	IVTEPC Ch1
GMT024	308.9	258.6	164.4	276.7	626.7	269.1
GMT025	436.3	402.8	240.1	411.6	914.0	408.4
GMT026	283.0	236.2	130.6	287.4	551.5	253.0
GMT027	225.6	41.0	115.3	65.9	504.7	348.2
GMT028	329.2	273.5	164.6	308.8	436.6	290.5

GCR Daily Dose [μGy]						
	SN1003	SN1004	SN1005	SN1007	SN1009	IVTEPC Ch1
GMT024	143.6	146.7	137.4	126.3	129.2	137.5
GMT025	139.7	106.5	135.0	122.3	129.3	134.0
GMT026	148.0	144.2	137.8	73.5	79.7	133.6
GMT027	124.3	60.6	43.8	86.3	106.9	132.4
GMT028	142.3	78.6	137.8	72.2	129.0	136.4
GCR Daily Dose Equivalent [μSv]						
	SN1003	SN1004	SN1005	SN1007	SN1009	IVTEPC Ch1
GMT024	430.5	468.1	405.8	486.9	443.8	448.8
GMT025	399.8	360.7	387.0	426.5	440.2	417.7
GMT026	483.9	485.1	404.5	260.8	278.2	410.0
GMT027	397.6	223.8	131.4	346.7	402.0	413.5
GMT028	405.4	228.2	401.7	236.8	467.2	432.4

Trapped Radiation Quality Factor						
	SN1003	SN1004	SN1005	SN1007	SN1009	IVTEPC Ch1
GMT024	1.8	2.0	1.9	1.8	1.8	1.7
GMT025	1.8	2.0	2.0	1.9	1.8	1.7
GMT026	2.0	2.0	1.8	1.8	1.9	1.7
GMT027	1.9	2.0	2.2	2.2	1.7	1.8
GMT028	1.8	2.0	1.9	2.0	1.8	1.8
GCR Quality Factor						
	SN1003	SN1004	SN1005	SN1007	SN1009	IVTEPC Ch1
GMT024	3.0	3.2	3.0	3.9	3.4	3.3
GMT025	2.9	3.4	2.9	3.5	3.4	3.1
GMT026	3.3	3.4	2.9	3.5	3.5	3.1
GMT027	3.2	3.7	3.0	4.0	3.8	3.1
GMT028	2.8	2.9	2.9	3.3	3.6	3.2

Percent Daily Coverage Trapped Radiation (relative to IVTEPC)						
	SN1003	SN1004	SN1005	SN1007	SN1009	IVTEPC Ch1
GMT024	100.00%	100.00%	100.00%	100.00%	100.00%	100.00%
GMT025	100.00%	100.00%	100.00%	100.00%	100.00%	100.00%
GMT026	100.00%	100.00%	100.00%	100.00%	100.00%	100.00%
GMT027	69.14%	12.35%	56.79%	22.22%	66.67%	100.00%
GMT028	100.00%	90.74%	100.00%	90.74%	100.00%	100.00%

Scaled Daily Trapped Radiation Dose [μGy]						
	SN1003	SN1004	SN1005	SN1007	SN1009	IVTEPC Ch1
GMT024	169.9	127.4	85.4	151.8	348.0	158.4
GMT025	244.8	199.8	119.4	220.1	495.2	237.3
GMT026	145.1	120.3	72.7	155.6	296.6	145.8
GMT027	175.6	167.3	93.0	136.9	441.7	192.9
GMT028	179.2	150.4	85.5	173.6	237.6	162.4
Scaled Daily Trapped Radiation Dose Equivalent [μSv]						
	SN1003	SN1004	SN1005	SN1007	SN1009	IVTEPC Ch1
GMT024	308.9	258.6	164.4	276.7	626.7	269.1
GMT025	436.3	402.8	240.1	411.6	914.0	408.4
GMT026	283.0	236.2	130.6	287.4	551.5	253.0
GMT027	326.3	331.9	203.1	296.4	757.0	348.2
GMT028	329.2	301.4	164.6	340.3	436.6	290.5

Percent Daily Coverage GCR (relative to IVTEPC)						
	SN1003	SN1004	SN1005	SN1007	SN1009	IVTEPC Ch1
GMT024	100.00%	100.00%	99.57%	100.00%	100.00%	100.00%
GMT025	100.00%	77.99%	100.00%	100.00%	100.00%	100.00%
GMT026	100.00%	100.00%	100.00%	64.77%	65.86%	100.00%
GMT027	87.20%	40.03%	37.45%	66.81%	87.12%	100.00%
GMT028	100.00%	58.01%	100.00%	61.62%	100.00%	100.00%

Scaled Daily GCR Dose [μGy]						
	SN1003	SN1004	SN1005	SN1007	SN1009	IVTEPC Ch1
GMT024	143.6	146.7	138.0	126.3	129.2	137.5
GMT025	139.7	136.6	135.0	122.3	129.3	134.0
GMT026	148.0	144.2	137.8	113.5	121.0	133.6
GMT027	142.5	151.4	116.9	129.2	122.7	132.4
GMT028	142.3	135.4	137.8	117.2	129.0	136.4
Scaled Daily GCR Dose Equivalent [μSv]						
	SN1003	SN1004	SN1005	SN1007	SN1009	IVTEPC Ch1
GMT024	430.5	468.1	407.5	486.9	443.8	448.8
GMT025	399.8	462.5	387.0	426.5	440.2	417.7
GMT026	483.9	485.1	404.5	402.6	422.3	410.0
GMT027	456.0	559.2	350.8	518.9	461.5	413.5
GMT028	405.4	393.4	401.7	384.3	467.2	432.4

REPORT DOCUMENTATION PAGE				Form Approved OMB No. 0704-0188	
<p>The public reporting burden for this collection of information is estimated to average 1 hour per response, including the time for reviewing instructions, searching existing data sources, gathering and maintaining the data needed, and completing and reviewing the collection of information. Send comments regarding this burden estimate or any other aspect of this collection of information, including suggestions for reducing this burden, to Department of Defense, Washington Headquarters Services, Directorate for Information Operations and Reports (0704-0188), 1215 Jefferson Davis Highway, Suite 1204, Arlington, VA 22202-4302. Respondents should be aware that notwithstanding any other provision of law, no person shall be subject to any penalty for failing to comply with a collection of information if it does not display a currently valid OMB control number.</p> <p>PLEASE DO NOT RETURN YOUR FORM TO THE ABOVE ADDRESS.</p>					
1. REPORT DATE (DD-MM-YYYY) 01-09-2016		2. REPORT TYPE Technical Memorandum		3. DATES COVERED (From - To)	
4. TITLE AND SUBTITLE Initial Report on International Space Station Radiation Environment Monitor Performance				5a. CONTRACT NUMBER	
				5b. GRANT NUMBER	
				5c. PROGRAM ELEMENT NUMBER	
6. AUTHOR(S) N. Stoffle, J. Keller, E. Semones				5d. PROJECT NUMBER	
				5e. TASK NUMBER	
				5f. WORK UNIT NUMBER	
7. PERFORMING ORGANIZATION NAME(S) AND ADDRESS(ES) NASA Johnson Space Center				8. PERFORMING ORGANIZATION REPORT NUMBER S-1228	
9. SPONSORING/MONITORING AGENCY NAME(S) AND ADDRESS(ES) National Aeronautics and Space Administration Washington, DC 20546-0001				10. SPONSOR/MONITOR'S ACRONYM(S) NASA	
				11. SPONSOR/MONITOR'S REPORT NUMBER(S) TM-2016-219278	
12. DISTRIBUTION/AVAILABILITY STATEMENT Unclassified-Unlimited Subject Category Availability: NASA STI Program (757) 864-9658					
13. SUPPLEMENTARY NOTES An electronic version can be found at http://ntrs.nasa.gov .					
14. ABSTRACT The International Space Station Radiation Environment Monitor (ISS REM) is a small, low-power, hybrid-pixel radiation detector based on the CERN Timepix technology. Five detectors were flown aboard ISS beginning in late 2012. This document contains the initial results from the first year of operation as reviewed in late 2013, including hardware issues, detector performance, and development efforts.					
15. SUBJECT TERMS Timepix, Ionizing Radiation, ISS					
16. SECURITY CLASSIFICATION OF:			17. LIMITATION OF ABSTRACT	18. NUMBER OF PAGES	19a. NAME OF RESPONSIBLE PERSON
a. REPORT	b. ABSTRACT	c. THIS PAGE			STI Information Desk (help@sti.nasa.gov)
U	U	U	UU	44	19b. TELEPHONE NUMBER (Include area code) (757) 864-9658

